

# Postural Hand Tremor and the Repetitive Photic Stimulation – A Coherence Joint Time Frequency Study

M.C. Dobra and D.M. Dobra

“Gh. Asachi” Technical University, Faculty of Electronics and Telecommunications, Iasi, Romania

**Abstract**— This study aims to shed light on physiological tremor signal – an output of the motor system whose origins and possible functional role are still not well understood. In order to uncover some potential hidden frequency relationship between the motor system output and, respectively, the visual system input – the last system being regarded as to bring the major sensory inputs from all sensory modalities – a repetitive photic stimulation paradigm was implemented. In order to prevent the cortical driven oscillations to interfere with the spontaneous cortical rhythm, the stimuli frequencies were particularly chosen out of the alpha frequency band. Particularly, two visual stimuli were used, being delivered at different frequency (7 Hz, 19 Hz) – either concurrently, either alternatively –, in each of the visual hemifield. The subjects were asked to look all the time at a fix central point while the steady state visual evoked potential was induced – by visual peripheral repetitive stimulation – along the visual path at both, cortical and, respectively, subcortical level. Physiological postural hand tremor was recorded bilaterally during the period of stimulation. Assuming that the visual influence could be induced in tremor signal through either the cortical or through direct subcortical paths – given the potential ability of most sensory neurons to access the motor neurons –, the relationship of the tremor waveform to the light flashes was further investigated. For this, the coherence function was calculated within a joint time-frequency analysis (JTFA) type, for all three hand signal combinations (left-right, left-left, right-right). The preliminary results show the existence of a light coherence at the frequency of interest. To validate these results further investigations will be done.

**Keywords**— Tremor, steady-state visual evoked potentials (SSVEPs), joint time-frequency analysis (JTFA), coherence

## I. INTRODUCTION

Hand tremor signals are not stationary processes [1] in a strict mathematical sense. Consequently, the spectra and the correlation functions calculated over some periods may reveal an intermittent dynamic relation. In this paper, in order to study the time-varying properties of the non-stationary hand-tremor signals we used an advancement of the linear Fourier transformation, namely, the continuous wavelet transform (CWT). In this case, the crucial issue of stationarity required by many time-series analysis methods was passed up. Moreover, the coherence function – a frequency domain method, employed using CWT – was used toward the identification of central modulating drives from physiological hand tremor (PT) recordings. The wavelet coherence (WTC) was implemented in two experimental

protocols investigating the visual influence assumed that had been induced in the PT signal through electroencephalographic (EEG) photic driving. Through this last method of experimental cortical activation, we attempted to modulate the central tremor-generating oscillators that likely contributed to the final generated PT, alongside the other assumed PT origins such as motor unit firing properties, mechanical resonances and reflex loop resonances. The central PT origin is the most recent promoted hypothesis among the PT multi-factorial origin theories. Related to this neurogenic origin several functional roles ascribed to the tremor were proposed, thus shifting the old viewpoint on the tremor regarded only as a source of unwanted noise in the motor system. These roles are reviewed in [2] and they are based on a cortical (central) – motor (peripheral) common rhythmicity that was confirmed by the presence of a synchronized discharge of corticomotor neurons at certain preferred frequencies [3]-[7]. Among the different peripheral synchronization patterns encountered in the limb – a) *short-term synchronization*, b) *external synchronization* and c) *long-term or broad-peak synchronization*, [2] –, the second type of synchronization (due to a common driving oscillator that also drives the descending inputs) is the only one that allows the investigator for an external noninvasive possible control in the tremor analysis methodology. Following these lines, a brain rhythm (SSVEP) was extrinsically driven through visual hemifield repetitive stimulation. Then, the presence of temporal (phase) relationship introduced between central induced oscillations and the peripheral tremor was further investigated. To do this we always kept in mind the correspondence existing, on one side, between each visual hemifield and its matching cortical activated hemisphere and, on the other side, between cortical activated hemisphere and its corresponding controlled limb (i.e. right visual hemifield – left visual cortical areas – right hand). Unlike the two previous communicated papers [8],[9] where the PT analyzed signals were acquired with the system proposed in [10] in this paper, in order to get comparable results with those reported in the literature, we developed and used a new accelerometer based tremor acquisition system. Besides the aim of revisiting the coherence function evaluation (as a method to explore how much the tremor signal is reflecting the synchronized cortical activity), two other objectives were proposed: a) to analyze the activation pattern of the two putative central oscillators proposed in [11] as independently controlling the right and left hands, and b) to search for some preferred coupling direction between these oscillators.

## II. MATERIALS AND METHODS

### A. Materials

The tremor acquisition system was implemented with two low-g accelerometer sensors (ADXL203, Analog Devices), a National Instruments data acquisition board (AT-MIO-16E-10) and a software program that acquired simultaneously, and in synchronism with the visual stimuli, the tremor signal of both hands. On a single chip, the ADXL203 circuit embeds a high precision, low power, dual axis iMEMS (integrated Micro Electro Mechanical System) accelerometer, that measures acceleration with a full-scale range of  $\pm 1.7$  g and a sensitivity of 1000 mV/g. The AT-MIO-16E-10 DAQ board was configured in the differential mode and acquired the tremor movement on 12 bits, with a sampling rate of 240 Hz. The low-pass filtering for anti-aliasing and noise reduction was implemented using the ADXL capability. The mass of the each accelerometer plus mounting plate was less than 5 g and the entire montage was positioned between the forefinger and the middle finger of the subject.

Two healthy right-handed adults, with normal or corrected-to-normal vision, served as volunteer subjects after giving informed consent. Their mean age was 30.1 (range 29 to 32) years. Additionally, they have been taken no kind of medication in the week previous to the recordings. All the recordings took place in a quiet room without any other source of light than that of the stimuli generator. The subjects were seated in front of a 17"-computer screen, the head stabilized with a chin rest at a constant viewing distance of 80 cm. Viewing was binocular and, during testing, the subjects had to maintain fixation on a central white cross while thinking at nothing and avoiding blinks or eye movements. They were instructed to use minimal effort to maintain their stretched hands in an approximately same horizontal position while having no visual control of them. For each subject and for each paradigm 40 trials were recorded, every trial taking 64 s. The elbows of the subjects were fixed and brief rests were allowed between each trial in order to avoid the arm fatigue influence.

In this study two different conditions were tested. In the 1<sup>st</sup> paradigm two stimuli were presented against a dark background at two different locations (left visual hemifield, LVH, and right visual hemifield, RVH). The stimuli were lined up along the horizontal meridian of a computer monitor set to a resolution of 1028 x 1024 pixels, with a refresh rate of 85 Hertz. Each stimulus was a white circle changing its luminosity between a black background and a white flash. Also, the stimuli subtended a viewing angle of 2.48 x 2.48 degrees, with an eccentricity of 10°12" representing the distance between the inner edges of the circles to the central fixation cross. The stimulus in each visual hemifield was flickered at a different frequency (with a 50/50 on/off cycle): the stimuli from the LVH was flickered at rate of 7 Hz and only in the first 32 seconds, while the stimuli from

the RVH was flickered at rate of 19 Hz and only in the last 32 seconds of a 64-seconds trial. Simultaneously with the stimuli the tremor signal from the both hands was recorded. In the 2<sup>nd</sup> paradigm the stimuli presented above were simultaneously delivered to the subject during all 64 seconds of a trial. Another difference is that after the first 32 seconds of the experiment the stimuli exchanged their frequency characteristics (now, left stimulus – 19 Hz, right stimulus – 7 Hz) and remained so until the end of the recording.

### B. Methods

Extensively applied to the study of neural activity, the coherence function is a frequency domain method that determines the degree of linear correlation between each frequency component of the two analyzed signals. Regarded as a measure of linear predictability, it equals one whenever one signal is obtained from the other one by a linear operator  $L(\cdot)$ . The general formula of the magnitude-squared coherence,  $\gamma_{xy}^2(f)$ , for a given frequency  $f$  and for two stationary random processes,  $x(t)$  and  $y(t)$ , is defined as the square of the cross spectrum,  $S_{xy}(f)$ , normalized by the individual auto spectra,  $S_{xx}(f)$  and  $S_{yy}(f)$ , as given in eq. (1):

$$\gamma_{xy}^2(f) = \frac{|S_{xy}(f)|^2}{S_{xx}(f) \cdot S_{yy}(f)} \quad (1)$$

As without any smoothing the coherence function will take an identical value of one at all frequencies [12], we calculated the pooled coherence estimate using the eq. (2). Hence, the signal-to-noise ratio is enhanced by signal averaging under the implicit assumption that the noise is a zero-mean random variable, independent of repetition. Here, the averaging was done across a number of repeated trials, without smoothing within trials:

$$\bar{\gamma}_{xy}^2(f) = \frac{\left| \sum_{l=0}^{N-1} \bar{S}_{xy}^l(f) \right|^2}{\left( \left[ \sum_{l=0}^{N-1} \bar{S}_{xx}^l(f) \right] \cdot \left[ \sum_{l=0}^{N-1} \bar{S}_{yy}^l(f) \right] \right)} \quad (2)$$

Thus, the coherence estimate between the two processes,  $x(t)$  and  $y(t)$ , is calculated over  $N$  realizations of the processes;  $\bar{S}_{xy}^l(f)$  is the cross-spectral density estimator;  $\bar{S}_{xx}^l(f)$  and  $\bar{S}_{yy}^l(f)$  are the auto-spectral densities estimates for the  $l$ th realization of each of the two processes. Due to Schwarz inequality the coherence function takes on a value between 0 (independence) and 1 (complete linear dependence).

In general, the estimates of the auto- and cross-spectra used in coherence formula are calculated using the Fourier analysis that, unfortunately, does not provide any information about the evolution of frequency components over time. In our case this limitation is overcome by using the *continuous wavelet transform* (CWT) that provides a *time-frequency representation* of the signals. It has the following two main advantages: a) an optimal resolution both, in time and in frequency domains, and b) the lack of the stationarity condition imposed to the signals. The CWT uses a family of ‘wavelets’ (dilated/contracted and shifted versions of a

unique *wavelet function*  $\psi(t)$ ); correspondingly, it gives a decomposition of  $x(t)$  in different scales (a collection of wavelet coefficients that are presented onto a continuous frequency range over  $t$ ), tending to be maximum at those scales and time locations where the wavelet best resembles  $x(t)$ . The CWT is given by the relations:

$$CWT_x(a, b) = \int_{-\infty}^{\infty} x(t) \psi_{a,b}^*(t) dt, \quad \psi_{a,b}^*(t) = \frac{1}{\sqrt{a}} \psi\left(\frac{t-b}{a}\right) \quad (3)$$

where:  $\psi(t)$  is called the mother wavelet,  $a$  is the scale and  $b$  is the translation parameter. To interpret the information produced by the CWT, the scale has to be converted into frequency [13], eq. (4), the last one being a physical notion more easily interpretable than the notion of scale:

$$CWT_x(a, b) = CWT_x(f, \tau) \Big|_{f=F_s \cdot f_0 / a, \tau=a} \quad (4)$$

Here,  $F_s$  is the sampling frequency,  $f_0$  represents the chosen central frequency of the wavelet energy spectrum,  $\tau$  represents the time and  $f$  is the pseudo-frequency corresponding to the scale  $a$ . By using the CWT, the obtained coherence function not only reveals the linear dependence that exists between two processes at a specified frequency, but it also indicates the very moment when it appears. Given 2 processes,  $x(t)$  and  $y(t)$ , and their time-frequency representations,  $CWT_x(f, \tau)$  and  $CWT_y(f, \tau)$ , we can rewrite the eq. (2) as:

$$\hat{\gamma}_{xy}^2(f, \tau) = \frac{\left| \sum_{l=0}^{N-1} \hat{S}_{xy}^l(f, \tau) \right|^2}{\left[ \sum_{l=0}^{N-1} \hat{S}_{xx}^l(f, \tau) \right] \cdot \left[ \sum_{l=0}^{N-1} \hat{S}_{yy}^l(f, \tau) \right]} \quad (5)$$

where:  $\hat{S}_{xy}^l(f, \tau) = CWT_x(f, \tau) \cdot CWT_y^*(f, \tau)$  is the time-frequency cross-spectrum, while  $\hat{S}_{xx}^l(f, \tau) = |CWT_x(f, \tau)|^2$  and  $\hat{S}_{yy}^l(f, \tau) = |CWT_y(f, \tau)|^2$  are the two auto-spectra.

The magnitude of the CWT coherence, called *wavelet coherogram*, can be graphically represented by 2D plots, with time on the horizontal axis, frequency on the vertical axis, and amplitude given by a gray-scale color, Fig. 1.

### III. RESULTS

The tremor signals were first pre-filtered with a FIR 45 Hz low-pass filter and de-trended, using a polynomial 2<sup>nd</sup> order for removing slow drifts introduced by the tremor acquisition systems. Our approach (CWT coherence analysis) was applied onto two sets of experimental data obtained within the already presented two different paradigms. Each of the two implemented paradigms generated two different *ensembles* of measurements (*realizations*) corresponding to the two random processes governing each individual hand tremor. Assuming the existence of the EEG induced steady-state visual evoked potentials and that of their modulating activity upon the central tremor-generating oscillators, we further hypothesized that, for each hand, evoked tremors

rhythms arose as a result of the ipsi-lateral repetitive visual hemifield stimulation. Correspondingly, pairs of concurrent tremors have been observed in both hands, with the temporal and pattern characteristics of the visual stimuli being marked in the data. Their analysis aimed to reveal the existence or not of an interaction between the two putative independent central oscillators. Also, in order to investigate the phase-locked phenomena likely generated in each hand tremor, pairs of distinct trials recorded for the same hand (left, respectively, right) and for the same presented stimuli and experimental conditions, were analyzed. Events of onset and cessation of any temporal relationship between the any two analyzed signals presented above were tracked and quantitatively characterized using CWT coherence; moreover, for this type of analysis, the temporal frequency-relationships information and their changes over time were integrated with the *a priori* knowledge regarding the temporal and pattern characteristics of the particular stimuli presented to the subject. Thus, it was expected that the coherence spectrum revealed magnitudes approaching 1 (black points in the coherogram) for those sections of the records where the two analyzed tremor signals concurrently shared the same significant spectral peaks (completely linear dependence) and magnitudes approaching 0 (white points in the coherogram) for those sections of the records where they had not significant peaks to share (linear independence of the signals). For computing the wavelet coherence we chose the complex Morlet wavelet, defined by the function:

$$\psi(t) = (1/\sqrt{\pi f_b}) \cdot \exp(2i \pi f_c t) \cdot \exp(-t^2/f_b) \quad (6)$$

As one can see, this wavelet depends on two adjustable parameters –  $f_b$  (a bandwidth parameter) and  $f_c$  (a wavelet centre frequency) –, their adjustment providing the possibility of selecting the time–frequency resolution suitable for a given signal. We set  $f_b = 0.5$  and  $f_c = 1$ ; the scale parameter  $a$  was chosen to take values within [5, 70] interval that corresponds to a frequency band of [3.43, 48] Hz. The wavelet coherence results indicated a similar behavior for both subjects. In Fig. 1 one can see the coherograms obtained for subject 1 and for both paradigms, after removing the insignificant peaks. Exactly, the coherence can be considered 95% significant only if it exceeds the threshold  $r_{95\%} = 1 - 0.05^{1/(N-1)}$  (with  $N$  representing the number of repeated trials on which the averaging was done) [14].

### IV. DISCUSSION

Parts of the acquired hand tremor signal are components derived inclusively from the respiratory movements and heart movements. For instance, the respiration contributes to the low frequency spectrum of the hand tremor signal, having a basic frequency around 0.1 up to 0.3 Hz for adult subject, with a band in the range of 0.05 to maximum 3 Hz. Hence, the coherence analysis was done beginning with frequencies above 3 Hz.

The results obtained for the rest of the frequency interval, up to 48 Hz, are somewhat inconclusive. First, no clear correlation exists between the significant coherence at the frequencies of interest (7 Hz, 19 Hz) and their corresponding delivery moments and affected hand. Additionally, the significant coherence values, that have an essential intermittent nature, span a large interval of frequencies, up to even 30 Hz, and only for the left-right hand pairs; this means that no phase-locked occurs at the hand PT level when visual stimuli are delivered. Moreover, the broad band significant coherence obtained for left-right pairs could signify some common central oscillations with a pervasive descending influence at the spinal level. Regarding the relative low values of the coherence function there are some possible reasons that should be considered. One of these could be a nonlinear relationship between the signals, which make the usual linear test useless.

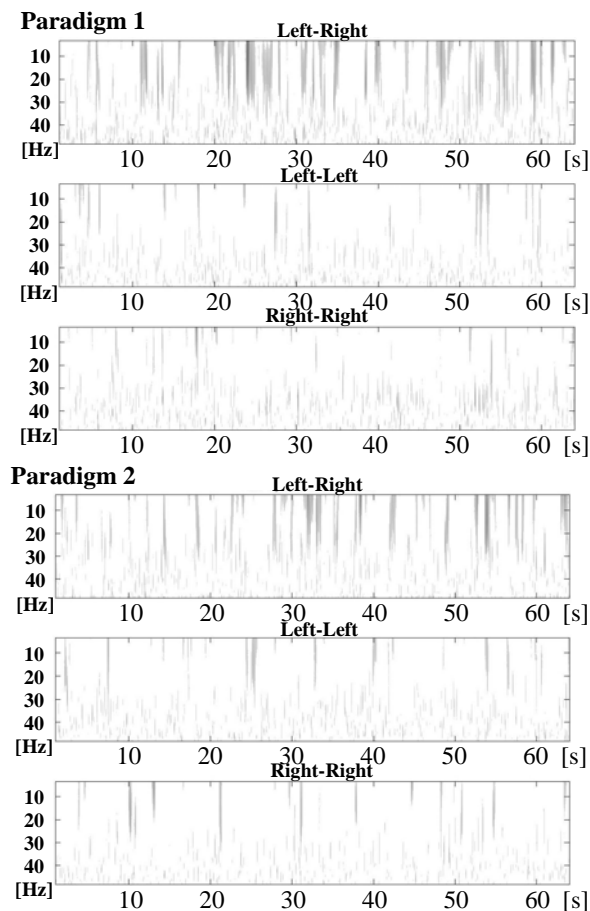


Fig. 1. The coherograms for subject 1

## V. CONCLUSIONS

The behaviour described above could: 1) confirm the hypothesis that the hand PT is not influenced by repetitive photic stimulation, or 2) the SSVEPs were not obtained as

expected, at the contralateral visual cortical level; this means that no central oscillators existed that could drive the hand tremor rhythms. It is known that the amplitude and phase of the SSVEPs are highly sensitive to stimulus parameters such as repetition rate, contrast or modulation depth etc. For a compelling analysis, a cortical activity monitoring (like EEG) is necessary in order to confirm and to allow the study of the central oscillators' activity as well.

## ACKNOWLEDGMENT

This work was supported by the Romanian National Council for Research in High Education, Grant Td, theme 103, code 145, 2006.

## REFERENCES

1. Moore G P, Ding L, Bronte-Stewart H M (2000) Concurrent Parkinson tremors. *The Journal of Physiology* 529.1: 273-281
2. McAuley J H, Marsden C D (2000) Physiological and pathological tremors and rhythmic central motor control. *Brain* 123: 1545 -1567
3. Ohara S et al (2000) Electrocochogram-electromyogram coherence during isometric contraction on hand muscle in human. *Clin Neurophysiol* 111: 2014 – 2024
4. Raethjen J et al (2003) Is the rhythm of physiological tremor involved in cortico-cortical interactions? *Mov Disord* 19 (4): 458 – 465
5. McAuley J H et al (1999) Human anticipatory eye movements may reflect rhythmic central nervous activity. *Neurosci.* 94(2): 339 – 350
6. McAuley J H et al (1997) Frequency peaks of tremor, muscle vibration and electromyographic activity at 10 Hz, 20 Hz and 40 Hz during human finger muscle contraction may reflect rhythmicities of central neural firing. *Exp Brain Res* 114 (3): 525 – 541
7. Vaillancourt D E, Newell K M (2000) Amplitude changes in the 8-12, 20-25, and 40 Hz oscillations in finger. *Clin Neurophysiol* 111 (10): 1792 – 1801
8. Serban M C, Dobrea D M, Teodorescu H N (2004) Evidence for the central oscillators in the physiological tremor generation process. CD-Proceedings of the 4th European Symp. In Biomed Eng, Session 4, Patras, Greece, 2004
9. Serban M C, Dobrea D M (2005) A phase analysis of the hand tremor signal in a photic driving paradigm, Proc of the 14th Int Conf of Med Phys, Nuremberg, Germany, 2005, pp. 1547-1548
10. Dobrea D M, Teodorescu H N, Mlynek D (2002) An interface for virtual reality applications. *Rom. J. of Inform Sci Tech.* 5(3): 269–282
11. Koster B et al (1998) Central mechanisms in human enhanced physiological tremor. *Neurosci Lett.* 241 (2-3): 135-138
12. Torrence C, Compo G P (1998) A practical guide to wavelet analysis. *Bulletin of the American Meteorological Society* 79(1): 61-78
13. Wang S - Y, Aziza T Z, Steina J F (2005) Time–frequency analysis of transient neuromuscular events: dynamic changes in activity of the subthalamic nucleus and forearm muscles related to the intermittent resting tremor. *Journal of Neuroscience Methods* 145: 151–158
14. Rosenberg J R et al (1989) The Fourier approach to the identification of functional coupling between neuronal spike trains. *Prog. Biophys. Mol. Biol.*, vol. 53, 1989, pp. 1-31

Address of the corresponding author:

Author: Monica-Claudia Dobrea (Serban)  
 Institute: "Gh. Asachi" Technical University  
 Street: Bd. Carol I no. 11  
 City: Iasi  
 Country: Romania  
 Email: serbanm@etc.tuiasi.ro